

# Wide Band Spurious Suppression of Multi-Strip Resonator BPF — Comprehensive Way to Suppress Spurious Responses in BPFs —

Ikuo AWAI<sup>†a)</sup>, *Fellow*

**SUMMARY** A new comprehensive method to suppress the spurious modes in a BPF is proposed taking the multi-strip resonator BPF as an example. It consists of disturbing the resonant frequency, coupling coefficient and external Q of the higher-order modes at the same time. The designed example has shown an extraordinarily good out-of-band response in the computer simulation.

**key words:** *spurious suppression, multi-strip resonator, BPF, LTCC structure*

## 1. Introduction

Band pass filters in the microwave frequency range are composed of connected resonators. They are usually designed by proper choice of the resonant frequency ( $f_r$ ), coupling coefficient ( $k$ ) and external Q ( $Q_e$ ) of the relevant resonators. But the distributed-element resonators for the higher frequency band such as the microwaves have infinite number of spurious modes in addition to the dominant mode that is used for the BPF pass band.

The present article proposes a new comprehensive method to suppress the spurious responses of a BPF, by applying the standard design rule destructively to the spurious modes. It means that one disturbs resonant frequency, coupling coefficient and external Q of the spurious modes from the optimal state, but keeps the optimal values for the dominant mode. There have been reported some independent detuning of one quantity among these three to the spurious modes. In fact, shift of the resonant frequency for the spurious modes in the neighboring dielectric resonators (DR) and stepped impedance resonators (SIR) have been shown effective in [1] and [2], respectively. Control of external Q was also tried for DRs successfully [2].

But our proposal is unique from those reports in that we start from the concept of total BPF design and apply the detuning to the spurious modes systematically. In order to do that, we find the parameter dependence of all three design parameters ( $f_r$ ,  $k$  and  $Q_e$ ) for the spurious modes in addition to the dominant mode [3].

The multi-strip resonators were proposed for miniaturization of resonators by our group [4] a few years ago. Their basic structure is the laminated interdigital metal strips fac-

ing their broad surfaces each other, which increases the mutual capacitance significantly, resulting in a very low resonant frequency. Thus, the original purpose of miniaturization has been attained. The unexpected side effects, however, were also found that the conductor Q of the resonator increases with the number of strips and the first spurious mode frequency goes apart from the dominant mode frequency with the narrower strip spacing. The latter will turn out to be useful for the end of the present article

The basic design concept is introduced first in this article, followed by the physical explanation of the electromagnetic field distribution of each mode. The design parameters  $f_r$ ,  $k$  and  $Q_e$  will be calculated by use of HFSS (Ansoft) for variety of dimensions of constituting metal strips. Some design examples will give the validity of the present method in the last.

## 2. Design of Pass Band and Spurious Bands

The fundamentals of BPF design are summarized in Table 1 by referring to the parameters to be determined. The operating conditions of a BPF in the left column determines the parameters of each resonator constituting the BPF in the right column.

The BPF design is usually carried out using the dominant mode of resonators to form the pass band, while the higher modes form spurious bands even if they are not optimally designed. The present proposal is to design the spurious bands as poor as possible intentionally, and delete those bands substantially.

In order to do that, we need to find the resonant frequency, coupling coefficient and external Q for the relevant resonant modes, including the spurious as well as the dominant modes.

### (1) Resonant frequency

The resonant frequency of each resonator constitut-

**Table 1** Correlation of parameters between BPF and resonators.

BPF	Resonators
Operating frequency	Resonant frequency
Bandwidth	Coupling coefficient
Matching with external circuit	External Q

Manuscript received April 16, 2010.

<sup>†</sup>The author is with Ryukoku University, Otsu-shi, 520-2194 Japan.

a) E-mail: awai@rins.ryukoku.ac.jp  
DOI: 10.1587/transle.E93.C.942

ing a BPF is made basically the same except small deviations due to the difference of coupling between the adjacent resonators. Thus, it will be appropriate to shift the resonant frequency of higher order modes in the spurious bands. Though the best choice to arrange the frequency is not known for now, the frequency should be different each other, at least. The way of changing the higher order mode frequency, while keeping the dominant mode frequency the same, depends on the types of resonator. In the present example, the number, width and overlapping length of strips could be varied.

(2) Coupling coefficient

According to the insertion loss method for the filter design, the coupling coefficient between resonators is specified depending on the number of resonators, fractional bandwidth and the type of BPF such as maximally flat, Chebyshev, and so on. While the dominant mode should obey the design rule, the higher order modes should couple each other weakly or irregularly. Though it is not known what irregularity is best for now, the low coupling coefficient as possible would be fine for the spurious mode suppression at least.

(3) External Q

The external Q ( $Q_e$ ) is the last parameter for the design of a BPF. After deciding the resonant frequency and coupling coefficient of each resonator,  $Q_e$  is chosen to match the BPF with the external circuits. Now,  $Q_e$  for the higher order modes should be irregular, again. "How irregular?" is the problem. Under the condition that the best solution is not known, it will be safe to choose the lowest coupling of the higher order modes to the external circuits, highest  $Q_e$  in other words.

This concept could also be applied for the other types of BPFs with the micro-stripline, coplanar line, waveguide resonators or even dielectric resonators.

3. Electromagnetic Field Distribution of Resonant Modes

The unit element for the multi-strip resonator shown in Fig. 1 is a strip quarter wavelength resonator. Thus, its resonant frequencies are  $f_0, 3f_0 \dots (2n-1)f_0 \dots$ , where  $f_0$  is the fundamental mode frequency. And we rename them as  $f_1, f_2, \dots, f_n \dots$ , respectively. If we have two strips of the same dimension interdigitally aligned, the original resonant frequencies split as  $(f_{11}, f_{12}), (f_{21}, f_{22}) \dots (f_{n1}, f_{n2}) \dots$ , respectively, where  $f_{11}$  and  $f_{12}$  are split frequencies from the origi-

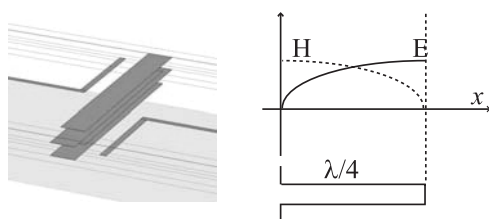


Fig. 1 Rough sketch of multi-strip resonator and longitudinal electromagnetic field distribution along one strip.

inal frequency  $f_1$ , for example. Now, when we couple strips with the number  $m$ , the resonant frequencies will be  $(f_{11}, f_{12} \dots f_{1m}), (f_{21}, f_{22} \dots f_{2m}), \dots (f_{n1}, f_{n2} \dots f_{nm}) \dots$ , respectively. We will call these groups the "family  $n$ ," and denote by  $M_n$ .

The longitudinal distribution of the electric field strength in a unit element of the multi-strip resonator is shown in Fig. 1. Since it does not change sign along the total length, the field distribution of the coupled strips may be represented by the signs + or - in Fig. 2. To take an example, Fig. 2(a) shows the odd and even mode in terms of the sign of electric field at each metal strip for the case of two strips. It is obvious that the odd mode has lower energy level, that is, lower resonant frequency than the even mode, and thus, mode names are given as  $M_{11}$  and  $M_{12}$ , respectively. The similar procedures have also been carried out for 3 and 4 strip cases, resulting in Figs. 2(b) and (c).

Now, the transverse electric field is depicted in Fig. 3 corresponding to Fig. 2(c) for the 4-strip case. The electric lines of force suggests the leaked electric field is stronger in the order  $M_{11} < M_{12} < M_{13} < M_{14}$ . Therefore, it will be expected that their electric coupling coefficient between adjacent two resonators should be in the same order.

Next, the magnetic field distribution will be examined corresponding to the sign of electric field in Fig. 2(c). The direction of current flow for each strip is drawn in Fig. 4.

It decomposes 4 strips and shows the direction of each current. Now, one reconstructs 4-strip resonator and looks at the magnetic line of force for each strip in the cross section to have Fig. 5. As an example,  $M_{11}$  has the same current direction for all strips, and hence, the magnetic field surrounds each strip in the same direction.

Figure 6 adds up all the magnetic field from each strips

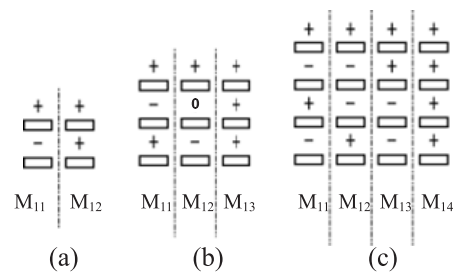


Fig. 2 Sign of voltage for eigen modes of resonator. (a) 2-strip resonator, (b) 3-strip resonator, (c) 4-strip resonator.

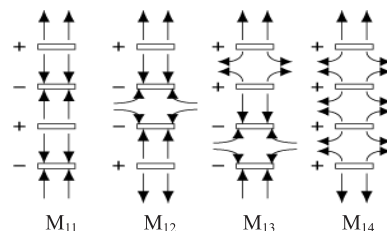


Fig. 3 Transverse electric field distribution for each mode in 4-strip resonator.

vectorially. Since the fields in  $M_{11}$  is added in the same direction, for example, the total outside field should be the largest, and the strength of external magnetic field may be ranked as  $M_{11} > M_{12} > M_{13} > M_{14}$ . It should be noted this order is just the opposite to that of the electric field. We have also calculated the transverse electro-magnetic field distribution with HFSS and shown them in Fig. 7, which confirms the qualitative consideration above. These electromagnetic field distributions will explain the coupling coefficient between adjacent resonators in Sect. 5.

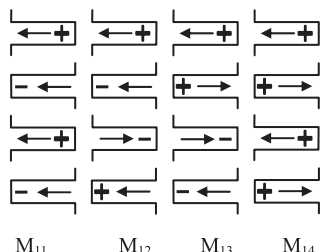


Fig. 4 Longitudinal direction of current induced by voltage shown in Fig. 2(c).

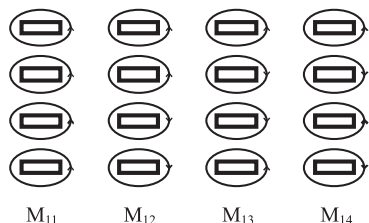


Fig. 5 Transverse magnetic field around each strip made by current shown in Fig. 4.

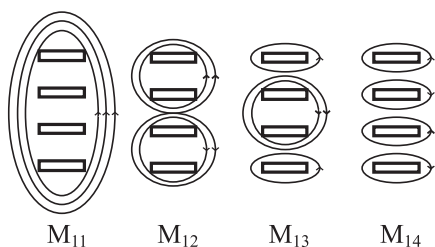


Fig. 6 Total transverse magnetic field around 4-strip resonator.

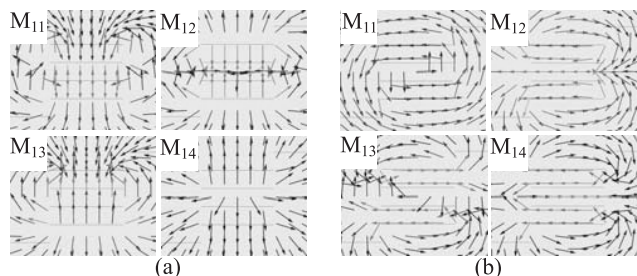


Fig. 7 Transverse (a) electric and (b) magnetic field calculated by E/M simulator HFSS.

#### 4. Resonant Frequency

The frequency splitting mentioned in the former section is numerically calculated and depicted in Fig. 8. The strip spacing is kept the same for each strip. It should be noted from Fig. 8 that,

- (1) the resonant frequencies of one  $\lambda/4$  strip resonator split into as many number of frequencies as the number of strips, and they are called to belong to a family.
- (2) the frequencies for different families do not mix even at the strongest coupling between strips. In other words,  $(f_{n1}, f_{n2} \dots f_{nm})$  are located adjacently, not mixed with  $(f_{n'1}, f_{n'2} \dots f_{n'm})$ .
- (3) the frequency difference between the adjacent members in certain family is almost the same irrespective of the strip spacing. In other words,  $f_{n1} - f_{n2}, f_{n2} - f_{n3}, \dots$  are almost the same.
- (4) the maximum splitting in a family is almost the same irrespective of the numbers of strips. In other words,  $f_{12} - f_{11}$  for 2 strips,  $f_{13} - f_{11}$  for 3 strips and  $f_{14} - f_{11}$  for 4 strips are almost the same in Fig. 8.

Looking at the frequency split shown in Fig. 8, we know that the resonant frequency of each mode for different number of strips would be different. In addition, when we compare the resonant frequencies of the spurious modes belonging to different families tuning the dominant mode frequency into the same value, we would see the disperse

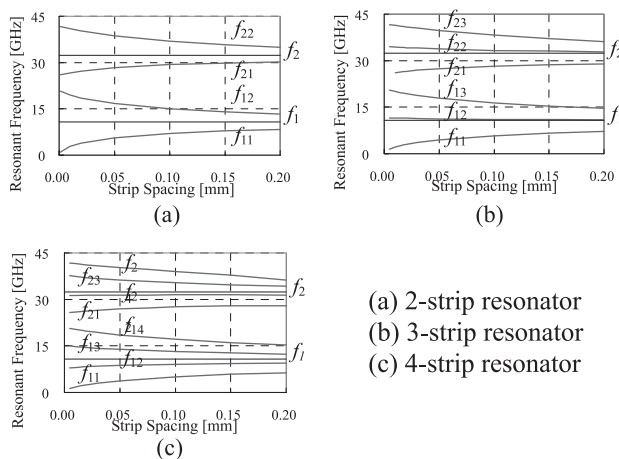


Fig. 8 Resonant frequencies of all modes versus strip spacing.

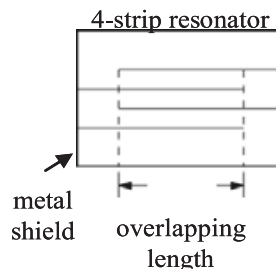
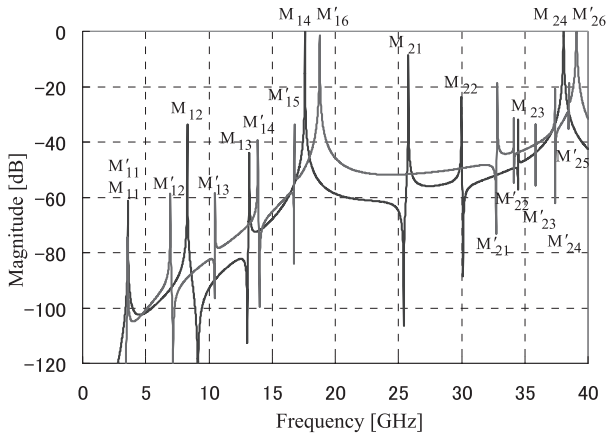


Fig. 9 Structure of 4-strip resonator to tune resonant frequency.

frequency distribution. If, for example, one equates the resonant frequency of each dominant mode  $M_{11}$  and  $M'_{11}$  for 4 and 6 layered resonators by adjusting the overlapping length of each resonator shown in Fig. 9, the other spurious modes such as  $M_{12}$ ,  $M_{13}$  get dispersed as shown in Fig. 10. The effect of the frequency detuning will be addressed in Sect. 7.

There is another method to disperse the spurious frequency of adjacent resonators. It is to prepare two resonators with different strip width. The resonant frequency



**Fig. 10** Resonant frequency of higher-order modes in 4 and 6 layered resonators with condition of same dominant mode frequency.

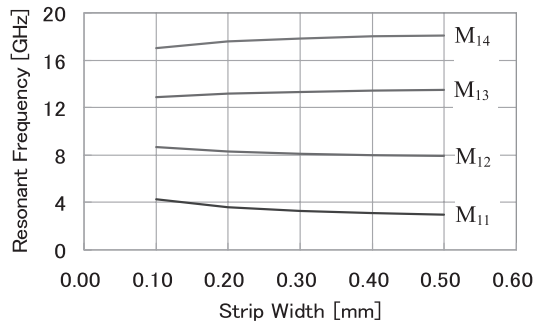


**Fig. 11** Resonant frequency of each mode for  $M_1$  family of 4-strip resonator vs. strip width.

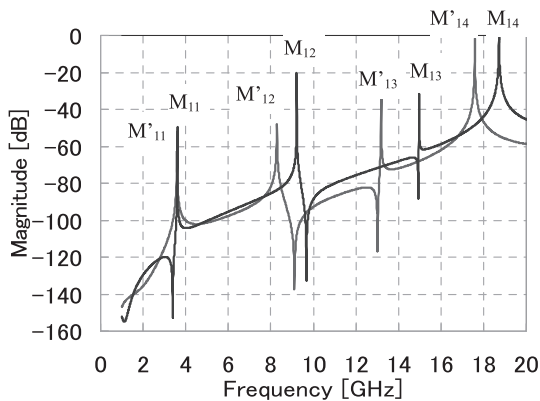


**Fig. 12** Resonant frequency of two 4-strip resonators with different width but same  $M_{11}$  frequency.

of  $\lambda/4$  strip that constitute a multi-strip resonator depends mainly on its length but also on its width a little, too. Besides that, the dependence is different among spurious modes. Therefore, two multi-strip resonators with different width have different distribution of resonant frequency for their spurious modes as shown in Fig. 11.

In Fig. 12, an example is shown that has the same resonant frequency for the fundamental mode, but different resonant frequency for the spurious modes between two resonators. Their strip widths are 0.2 and 0.4 mm, while strip lengths are 1.6 and 1.4 mm, respectively. The tuning of fundamental mode frequency is carried out by adjustment of overlapping length of multi-strips in the same manner as the former case (Fig. 9). It is needless to say that adjustment of overlapping length results in slight change of strip length.

**5. Coupling Coefficient**

The coupling coefficient between resonators is divided into the magnetic and electric components,  $k_m$  and  $k_e$ , respectively. They are subtracted each other to make the total coupling [5]

$$k = k_m - k_e \tag{1}$$

Now, the electric and magnetic field distribution in Figs. 3 and 6 is used to estimate the coupling coefficients of each mode in the family  $M_1$ . According to Fig. 3, the external electric field is strongest for  $M_{14}$  and weakest for  $M_{11}$ . Thus, the electric coupling should be large in the order  $M_{11} < M_{12} < M_{13} < M_{14}$ . On the other hand, Fig. 6 suggests that the magnetic coupling should be large in the order  $M_{11} > M_{12} > M_{13} > M_{14}$ . Thus, the rough insight into spurious suppression will be given in Fig. 13. It indicates the magnetic and electric components for each mode and the total coupling coefficient  $k$  with the hatched part. One expects larger  $k$  for  $M_{11}$  and  $M_{14}$ , while smaller  $k$  for  $M_{12}$  and  $M_{13}$ . Judging from its magnitude for each mode,  $M_{12}$  and  $M_{13}$  will be expected to be suppressed.

In order to estimate the coupling coefficient more quantitatively, one can use the perturbation method [5]. The numerically calculated results are shown in Fig. 14. Though the magnitudes of the coupling coefficient are not necessarily compared well, the qualitative property has been satisfactorily predicted by the physical consideration, including the separated magnetic and electric coupling coefficients.

It is concluded that the modes with either the smallest

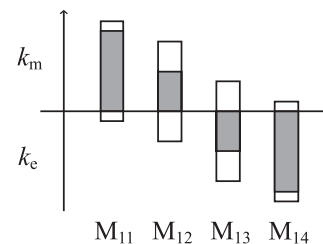


**Fig. 13** Coupling coefficient determined by Eq. (1).

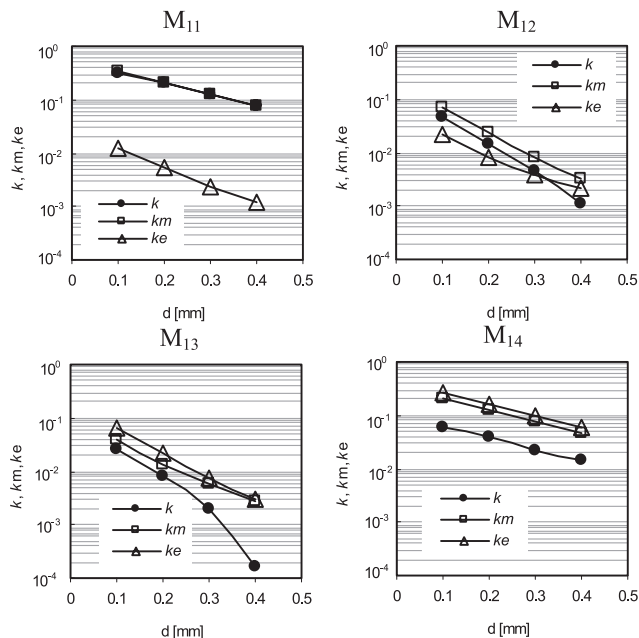


**Fig. 14** Numerically calculated coupling coefficients by E/M simulator HFSS.

or largest member number has the large coupling coefficient, while the other members with intermediate numbers do not. Specifically,  $M_{11}$  and  $M_{14}$  have large  $k$ , but  $M_{12}$  and  $M_{13}$  do not for the 4-strip resonator. This property is also true for resonators with other number of strips.

**6. External Q**

External  $Q$  is chosen to match the BPF with the external circuit. The calculated  $Q_e$  is shown in Fig. 15 as functions of the excitation line length along the strips in Fig. 1. Though  $Q_e$  should correspond to the coupling coefficient of  $M_{11}$  for good BPF matching, it should be quite different from the good matching for the spurious modes. Since the value for  $M_{14}$ ,  $M'_{16}$  vary with a big range in Fig. 15, we may be able to make use of it.

Now, let us make a digression. Though the external  $Q$  is widely used for BPF design, it is for adjusting the coupling to the external circuits with the outermost resonators in order to attain the circuit matching. The quantity  $Q_e$  was probably introduced in analogy with unloaded  $Q$  ( $Q_u$ ) which is the reciprocal of loss in a resonator. In fact, the reciprocal of  $Q_e$  shows the loss in external circuits. But in spite of the fact that  $Q_u$  represents the quality of a resonator,  $Q_e$  does not at all, but it represents the coupling to the external circuits.

Thus, we would like to introduce the external  $k$ ,  $k_x$  instead of  $Q_e$  as its reciprocal. This quantity is quite convenient to compare the coupling of the outermost resonator to the external circuit for various resonant modes. Besides that, its common use for BPF design at large will give simpler understanding that stronger coupling between resonators requires stronger coupling to the external circuits.

The  $k_x$  for 4 and 6-layered resonators is depicted in

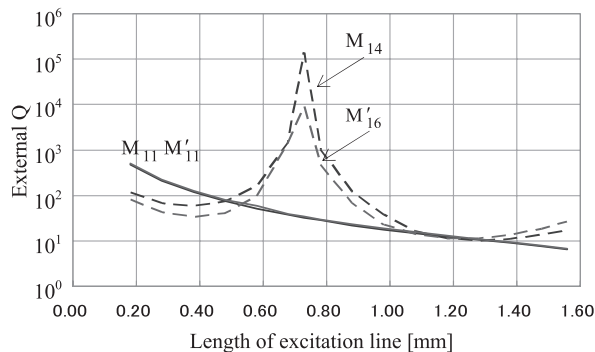


**Fig. 15** External  $Q$  of  $M_{11}$ ,  $M'_{11}$ ,  $M_{14}$  and  $M'_{16}$  modes vs. length  $l$  of excitation line along strips.

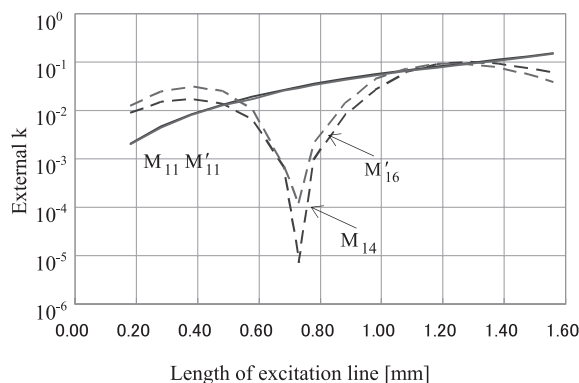


**Fig. 16** External  $k$  of  $M_{11}$ ,  $M'_{11}$ ,  $M_{14}$  and  $M'_{16}$  modes vs. length of excitation line along strips.

Fig. 16 as the reciprocal of Fig. 15. The significant feature is that  $k_x$  becomes zero for  $M_{14}$  and  $M'_{16}$  at some length of the external coupling line. It may be due to cancellation of magnetic and electric coupling just as the case in coupling between resonators. Since this sort of phenomenon has never been reported, it needs to be clarified as soon as possible.

Getting back to the trace, it is necessary to vary  $k_x$  for the dominant mode according to the demand for variety of bandwidth, though small  $k_x$  for the spurious modes will be effective for their suppression. For the excitation scheme shown in Fig. 1, shift of the excitation line perpendicularly to the resonator controls  $k_x$  for the dominant modes  $M_{11}$  and  $M'_{11}$  while keeping that for the spurious modes  $M_{14}$  and  $M'_{16}$  quite small. But this procedure will be omitted this time because the frequency detuning is enough to suppress  $M_{14}$  and  $M'_{16}$  modes as is seen in Figs. 10 and 12.

**7. Design Examples**

We will show three examples to confirm the validity of the proposed method of spurious suppression. Since the agreement between the simulation and experiment has been demonstrated already [6], [7], we will only show the simulation results here. In the first and second examples, one uses only detuning of the resonant frequency. The third example

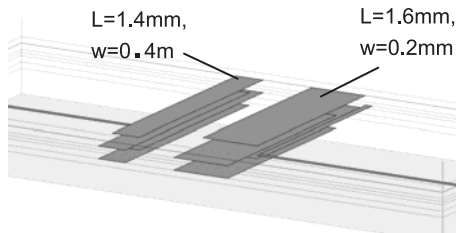


Fig. 17 Configuration of 4-strip resonator BPF with different strip width.

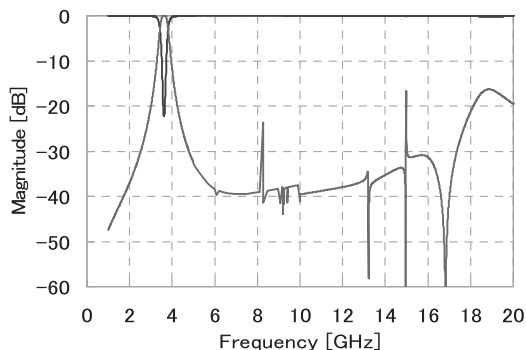


Fig. 18 Frequency response of 2-stage BPF made of 4-strip resonators with different strip width.

relies on mismatching of the external  $k$  as well as the resonant frequency. The small coupling coefficient for some of the spurious modes is always maintained, and hence we can expect those modes are always suppressed.

(1) Frequency detuning 1

In Fig. 17, frequency detuning is carried out by changing the width of adjacent resonators along the line shown in Figs. 11 and 12. Two resonators with the width 0.2 mm and 0.4 mm are used for 2-stage BPF, and give the frequency response shown in Fig. 18. Sizable improvement of the spurious suppression is noted. Though there are seen some sharp spikes of  $S_{21}$ , they will disappear by introduction of practically existing dielectric and conductor loss.

(2) Frequency detuning 2

Another way of frequency detuning could be adopted as shown in Figs. 8 and 10. It is to change the number of strips, causing the same effect as the former example. The present BPF is fabricated by 4 and 6-strip resonators, its frequency response being shown in Fig. 19. Since the resonant frequencies are dispersed as described in Fig. 10, the spurious modes are suppressed quite extensively.

(3) Mismatching of  $k_x$  as well as frequency detuning

If we determine that the suppression of the highest mode (around 20 GHz) of  $M_1$  family is insufficient in Fig. 19, we will introduce another measure, circuit mismatching, explained in Fig. 16.

Using the external line length 0.72 mm in Fig. 16, we have very small coupling of  $M_{14}$  and  $M'_{16}$  modes to the external circuits, while keeping the reasonable  $k_x$  for the dominant  $M_{11}$  and  $M'_{11}$  modes. Thus, we have designed an extremely wide spurious suppression through 40 GHz as is de-

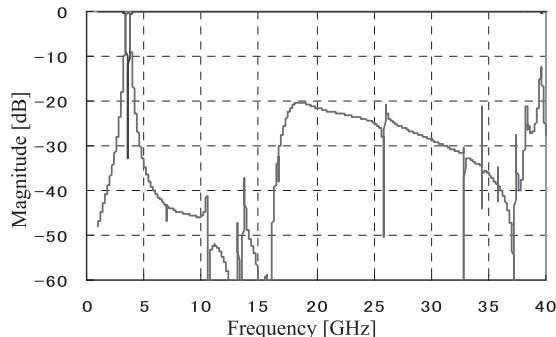


Fig. 19 Frequency response of 2-stage BPF made of 4- and 6-strip resonators.

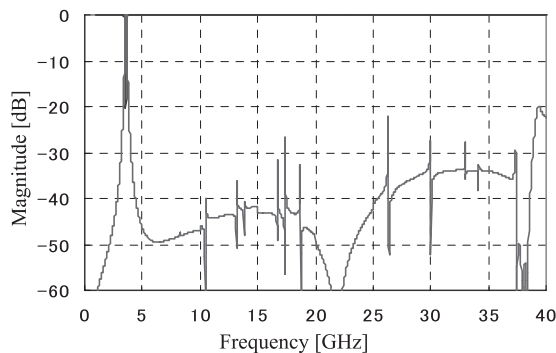


Fig. 20 Frequency response of 2-stage BPF made of 4- and 6-strip resonators with external coupling adjusted.

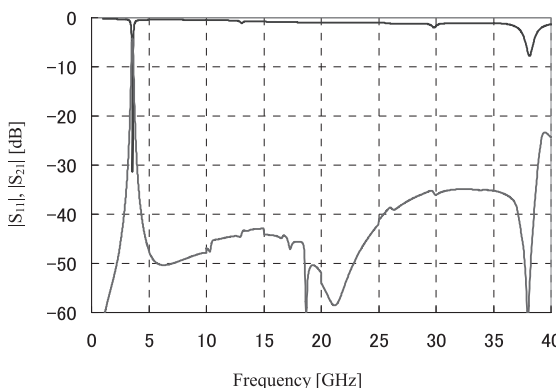


Fig. 21 Frequency response of 2-stage BPF made of 4- and 6-strip resonators with external coupling adjusted and loss introduced.

picted in Fig. 20. Many small spikes in  $S_{21}$  disappear by introduction of conductor and dielectric loss of the material in the simulation as shown in Fig. 21.

8. Conclusion

A comprehensive method to suppress spurious response in a BPF has been proposed taking multi-strip resonator BPF as an example. It is the combination of the resonant frequency detuning, coupling coefficient minimizing and external circuit mismatching for the spurious modes. In order to do that, the resonant frequency, coupling coefficient and external Q

of the spurious modes are to be obtained for various configurations and/or dimensions of constituting resonators. Good combinations of three measures mentioned above will give a satisfactory suppression.

Three design examples give the validity of the proposed design method, and its basic concept could be applied to variety of resonator filters.

The author appreciates the simulation works by Mr. T. Ishitani with Hirai Seimitsu Co. and the support by Ryukoku University.

## References

- [1] J.T. Kuo and H.P. Lin, "Dual band bandpass filter with improved performance in extended upper rejection band," *IEEE Trans. Microw. Theory Tech.*, vol.57, no.4, pp.824–829, April 2009.
- [2] T. Yamakawa, T. Yamada, T. Ishizaki, and A. Enokihara, "Dielectric filter," Patent, PCT/JP00/07643, May 2000.
- [3] I. Awai, T. Ishitani, and M. Fujimoto, "Multi-strip resonator BPF with extended spurious suppression in LTCC structure — Proposal of new concept to suppress spurious response in BPF," *Proc. APMC 2009, WE1C-4*, Singapore, Dec. 2009.
- [4] I. Awai, M. Inoue, Y. Maeda, T. Fukunaga, Y. Murabayashi, and M. Fujimoto, "Novel multi-strip resonator and filter," *Proc. 38th EuMC*, pp.1406–1409, Amsterdam, Oct. 2008.
- [5] I. Awai and Y. Zhang, "Coupling coefficient of resonators — An intuitive way of its understanding," *IEICE Trans. Electron. (Japanese Edition)*, vol.J89-C, no.12, pp.962–968, Dec. 2006.
- [6] I. Awai, Y. Maeda, D. Hanatani, and M. Fujimoto, "Multi-strip LTCC resonator BPF," *IEICE Electronics Express*, vol.5, no.22, pp.978–982, Nov. 2008.
- [7] I. Awai, T. Ishitani, Y. Zhang, D. Hanatani, and M. Fujimoto, "Spurious characteristics of multi-strip resonator BPF," *Proc. KJMW2009*, pp.1–4, Jeju, Korea, April 2009.



**Ikuo Awai** received the B.S. degree in 1963, M.S. degree in 1965, and Ph.D. in 1978, all from Kyoto University, Kyoto, Japan. In 1968, he joined Department of Electronics, Kyoto University, Japan, as a research associate, where he was engaged in microwave magnetic waves and integrated optics. From 1984 to 1990, he worked for Uniden Corporation, Japan, developing microwave communication equipments. He joined Yamaguchi University as a professor in 1990, where he has studied magnetostatic wave

devices, dielectric wave-guide components, super-conducting devices and artificial dielectric resonators for microwave application. In 2004, he started to work for Ryukoku University as a professor, being mainly engaged in microwave filters, meta-materials and wireless power transfer. He received the paper award from IEICE in 2002. He served as the chair of the Technical Group on Microwaves, IEICE, the chair of IEEE MTT-S Tokyo Chapter, Kansai Chapter and the chair of IEEE Hiroshima Section. Dr. Awai is a Fellow of MTT society of IEEE.